

UNIVERSITY of CALIFORNIA
SANTA CRUZ

**On the Distinction between Low Mass Brown Dwarfs and High Mass
Planets**

A Thesis Submitted in Partial Satisfaction
Of the Requirements for the Degree of

BACHELOR OF SCIENCE
in
ASTROPHYSICS

by
Bryce Harling
March 17, 2014

Professor Jonathan Fortney
Advisor

Professor Adriane Steinacker
Senior Theses Coordinator

Professor Michael Dine
Chair, Department of Physics

On the Distinction between Low Mass Brown Dwarfs and High Mass Planets

by Bryce Harling

ABSTRACT

In this paper we look at the traditional distinction between high mass gas planets and low mass brown dwarfs and note how the current definitions do not do enough to distinguish the two objects. We propose looking at the formation scenario of an object to determine its status as a planet or brown dwarf, and suggest observational ways to achieve this goal.

Contents

1.0	Introduction	1
2.0	Gravitational Instability Models	5
3.0	Core Accretion Models	16
4.0	Observations	25
	4.1 Observation of Core Accreted Objects	25
	4.2 Observations of Brown Dwarfs	27
5.0	Conclusion	30
	Acknowledgments	31
	References	32

1.0 Introduction

Planetary discovery has progressed from front page news to a routine endeavor, as over one thousand planets have thus far been confirmed. When people first looked into the night sky it was easy to distinguish planets from stars, as the planets slowly moved across the sky. In the 1990's we began to look outside our own solar system to find planets and with this came a need for a more specific definition of a planet. Some of the first objects found were massive, much larger than any object in our own solar system. This raised a question of where the definition of a planet ended. The next object on the mass scale is called a brown dwarf. Brown dwarfs are believed to form like stars, but are not massive enough to maintain hydrogen fusion throughout their lifetime. And so we found out that the smallest of these failed stars, and these massive planets have a mass regime that overlaps.

When brown dwarfs were initially discovered it was shown that they could in fact fuse some materials including deuterium and lithium, and that was the initial definition of a brown dwarf. As planetary models evolved, and scientists realized how massive planets could get, it was shown that planets could eventually fuse deuterium as well! So we have two distinctly different objects that overlap in mass, and can fuse the same materials. Both of the initial definitions of a planet and brown dwarf weren't distinct enough to distinguish a large planet from a small brown dwarf. However further research in both planetary sciences, and brown dwarf formation has led us to believe that each object forms in a distinctly different manner. This paper looks to describe initial formation scenarios of each object, and the need to establish the initial formation condition as the only sufficient way to define an object as a brown dwarf or planet.

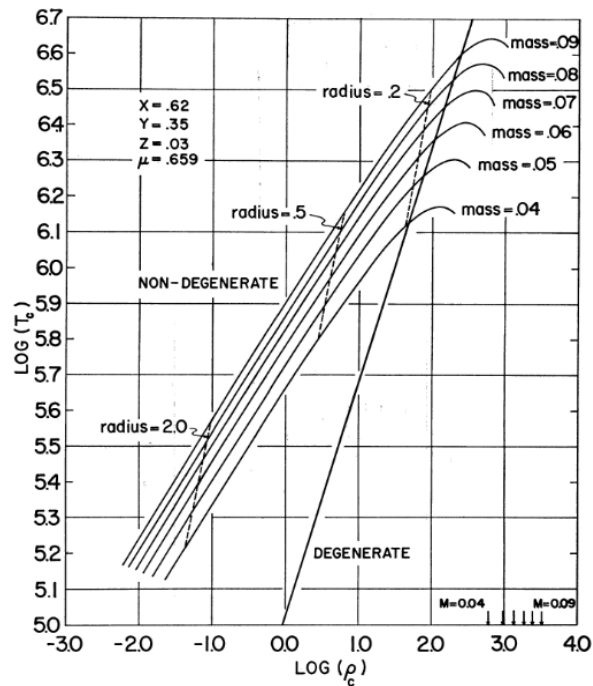


Figure 1: Temperature density diagram of the first modeled brown dwarfs. Mass and Radius are in solar units. The solid linear line represents where the matter will become degenerate. Were these objects able to continue to fuse elements, they would flatten at their peaks. Instead they begin to fall when they can no longer sustain fusion. (Kumar, 1962)

Brown dwarfs were first discussed as a possibility by Kumar in 1962. He constructed a convective model of low mass stars which first revealed the possibility of an object about 95 Jupiter masses, or M_J , initially igniting deuterium, or heavy hydrogen, then not having sufficient mass to continue fusion of heavier elements, before cooling to a planet-like object. We can see in figure 1 how these brown dwarfs vary from the traditional stellar path, and begin to cool after the gravitational force can no longer overwhelm the pressure force. The figure shows that a brown dwarf follows the path of a star rising in temperature and density as it contracts. As it begins to fuse deuterium the temperature and radius increases until a point at which the brown dwarf is not massive enough to continue down the fusion chain. At this point, where the internal matter begins to become degenerate, the brown dwarfs start to cool, and over the course of a few billion years will shrink to a radius within a few percentage of R_J , or the radius of Jupiter.

Because of this feature, brown dwarfs are very difficult to detect as they are bright for a very short period of time. They remained a theoretical possibility until 1995 when the first brown dwarf was discovered (Nakajima et al 1995).

Brown dwarfs are, in essence, the tail end of stars. They exist in the mass range with a lower limit of about $13 M_J$ up to $80 M_J$. On the low mass end, they begin to fuse deuterium, or heavy hydrogen, while around $65 M_J$ and above they will ignite lithium. It is simple to distinguish a brown dwarf from a star, as a star will reach the main sequence and begin to fuse hydrogen. It is around the lower limit of about $13 M_J$ where questions arise on how to determine the difference between a very-low-mass brown dwarf and a large gas giant.

A brown dwarf forms in a very similar manner to a star. A small part of a molecular cloud with inconsistent density can collapse into a brown dwarf. Many times this occurs in the same locations of star formation. In this process the mass of the collapsing cloud of gas will overcome the internal pressure of the object and can begin to fuse deuterium (Spiegel, Burrows, Milson 2010). The mass at which deuterium is fused can range due to the initial metallicity content, or amount of heavy elements, of the parent nebula, ranging from $12M_J$ to $14.5M_J$.

A planet forms through the process called core accretion. Around a protostar exists a protoplanetary disk. In this disk, grains can collide with one another to create a metallic core. This core can then travel through the rest of the disk and gather more material, eventually ending in a large gas planet. This formation tends to occur at a quick rate, as it can only accrete mass while the planetary disk exists, possibly on the timescale of a few millions years. Deuterium burning can occur at a low mass, closer to $12.5 M_J$ (Bodenheimer et al 2013).

The first section of this paper will cover the models proposed to simulate the formation of low mass brown dwarfs. Section three will look at the core accretion model. Section four will contain information on how these $13M_J$ objects are observed, and what to look for to distinguish their formation conditions. The final section will include an analysis and conclusion of what limit defines a brown dwarf in comparison to a large gas giant.

2.0 Gravitational Instability Models

As mentioned in the introduction, Shiv S. Kumar first postulated the existence of brown dwarfs in 1963. He began by modeling low mass stars with one of two compositions: $X=.90$, $Y=.09$ and $Z=.01$ a star of low metallicity, and $X=.62$ $Y=.35$ $Z=.03$ a star with much higher metallic levels. In these models $X+Y+Z=1$, where X is the hydrogen mass fraction, Y is the helium mass fraction, and Z represents all heavier elements. With these two populations he discovered that these low mass stars reached a maximum temperature and luminosity not high enough to sustain hydrogen fusion, after which they began to cool and shrink. This was the first time someone had tested what would occur when an object formed at sub-stellar masses.

More focus began to be put on these substellar objects and in 1975 Jill Tarter coined the term “brown dwarf” to describe these failed stars. As more effort was put in to understand the formation processes of these objects a better picture of their lifetime was created. The following figure, from Burrows et al (2001), displays the luminosity of a brown dwarf over time.

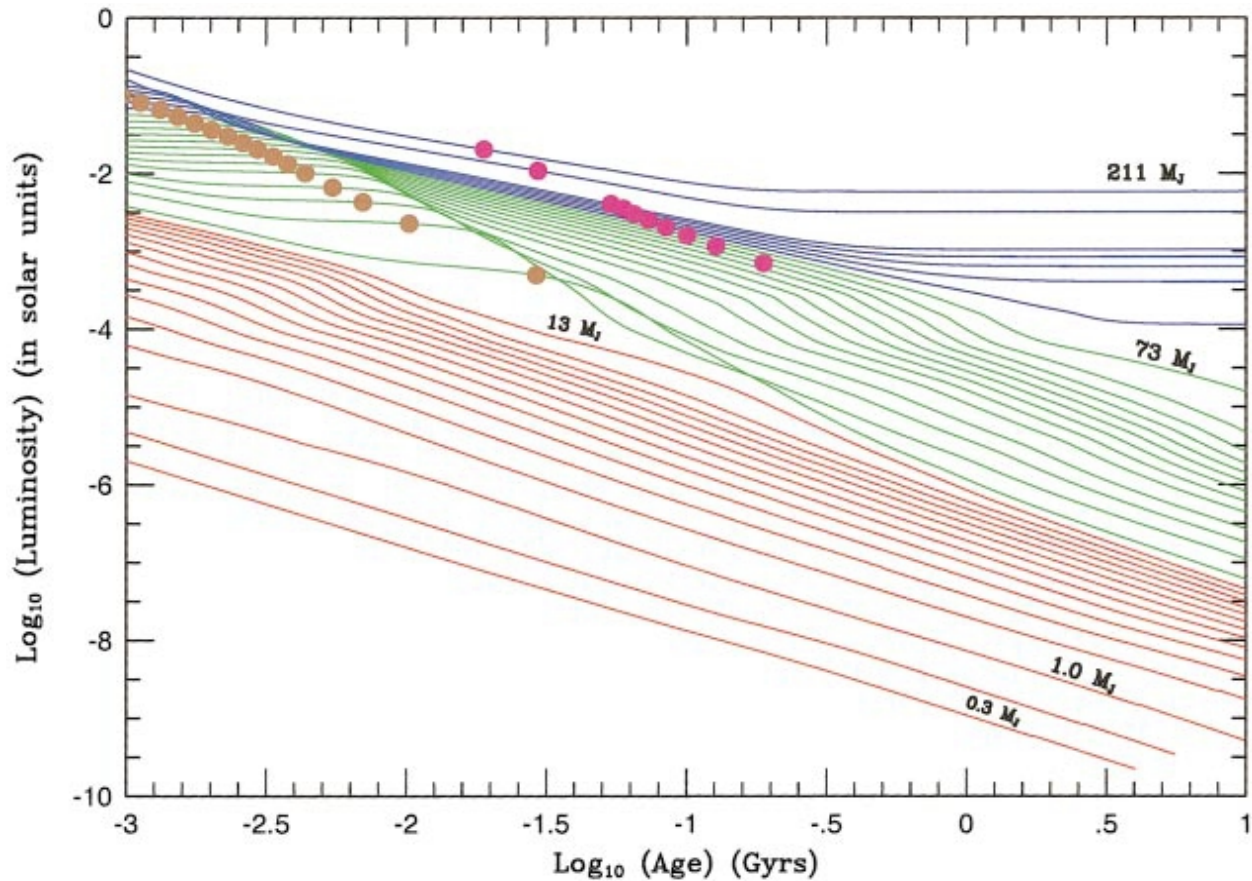


Figure 2

In this figure blue lines represent objects that are on the order of the smallest possible stars, about $75 M_{\odot}$. That is they have sufficient mass to fuse hydrogen, halting their contraction and continue onto the main sequence. The green line represents objects above $13 M_{\odot}$, while objects below that mass are illustrated in red. The gold dots show when 50% of the deuterium has been fused, and the magenta dots show where 50% of the lithium has burned. It is important to note the plateau effect of the luminosity, as this is a result of deuterium burning. It is most pronounced on the last green line, as the larger mass brown dwarfs burn the available fuel much faster. This is apparent in the following figure from G. Chabrier (2000) which shows different brown dwarf initial masses as a function of age and the brightness in the infrared.

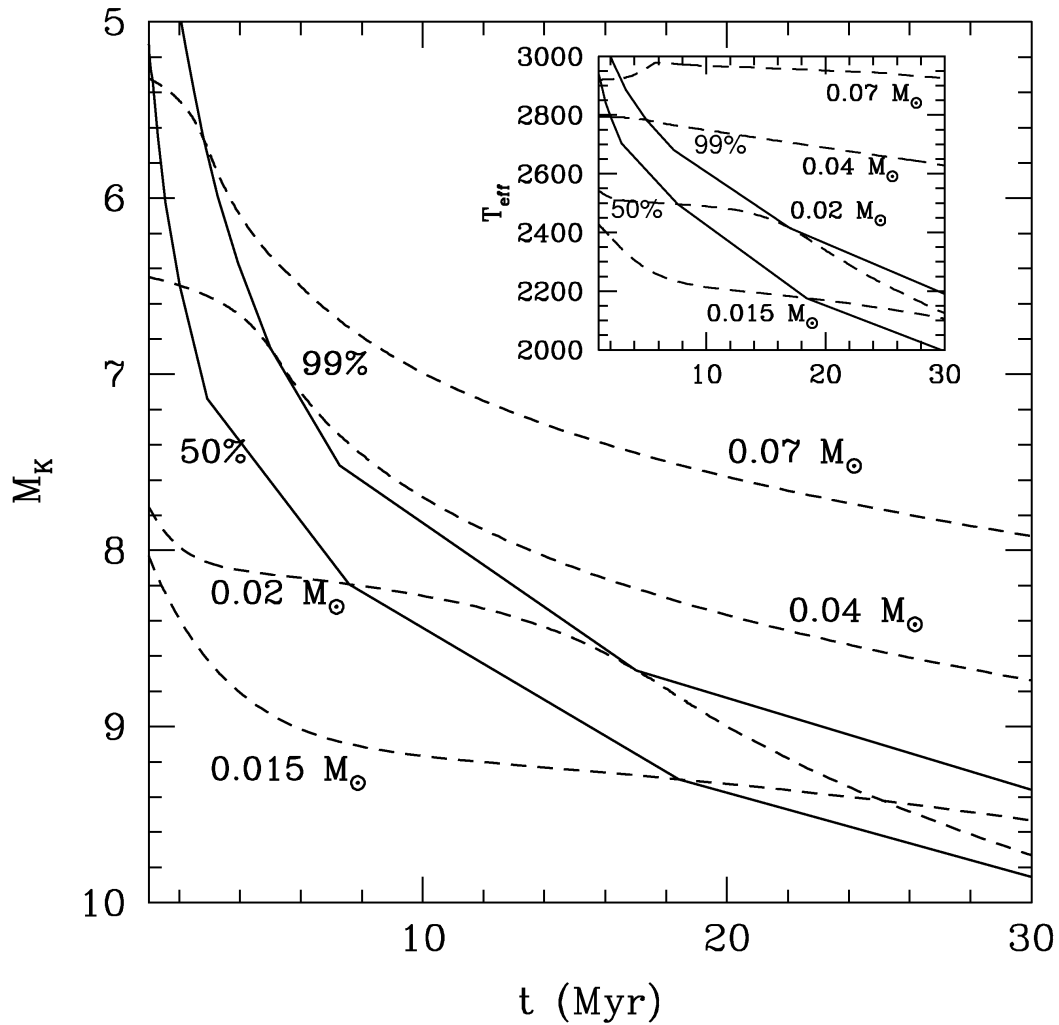


Figure 3

Here the solid lines represent the amount of deuterium burned with 99% the upper line and 50% the lower. The dashed lines represent the different starting masses for the modeled brown dwarfs. The dashed lines are equivalent to $73M_J$, $42M_J$, $21M_J$, and $16M_J$ respectively. Here we can see the time it takes the largest object to burn only one ninth the time for the smaller object. The inset shows the same masses as a function of age and effective temperature.

The initial mass of a brown dwarf has effects on its temperature as a function of time. More massive brown dwarfs are always hotter at a given age, and therefore burn their deuterium faster. After burning all available fuel, it will shrink, and cool. Smaller

objects will also see a short-term increase of temperature, however at a much smaller scale. The following figure, also take from Burrows (2001) helps to demonstrate this with the same population as figure one.

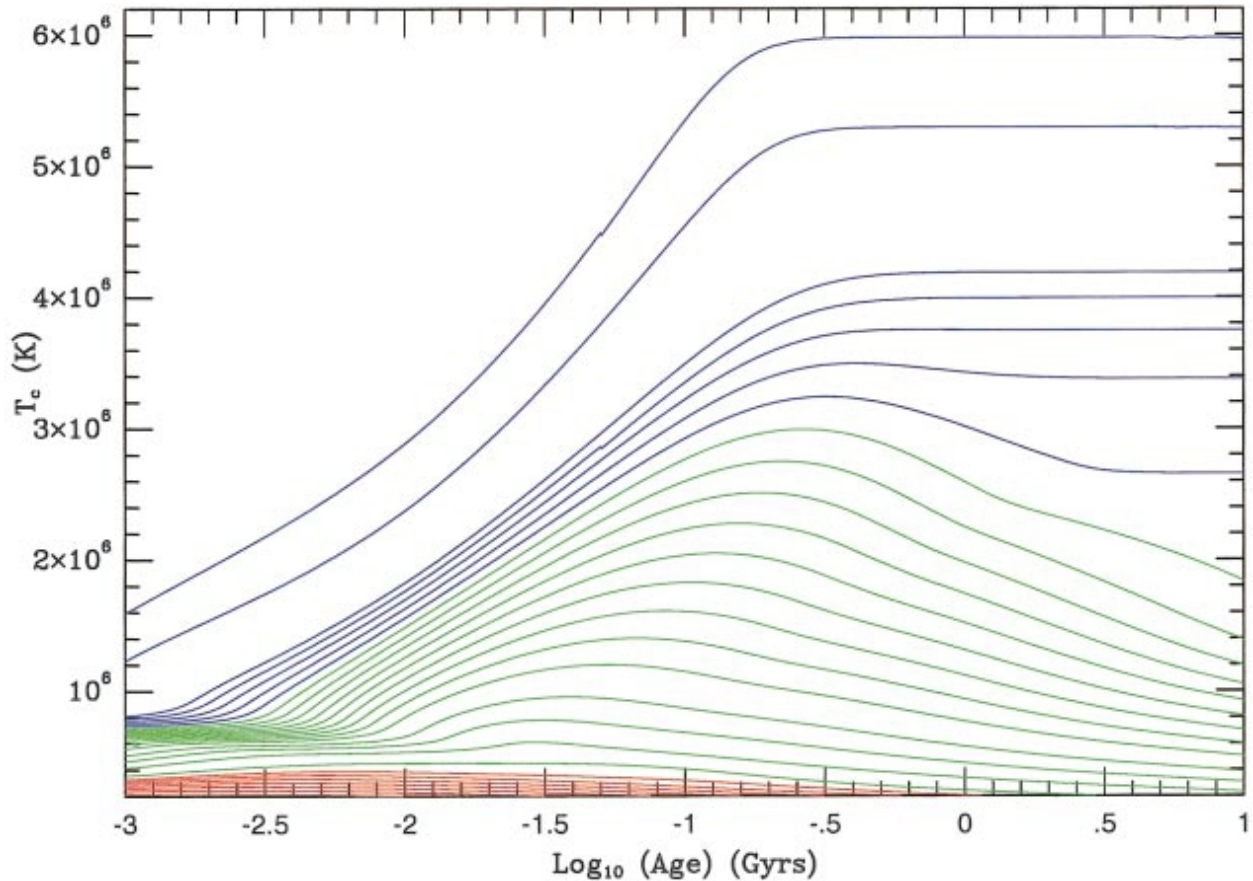


Figure 4

By comparing the two graphs, we can see that the maximum temperature is concurrent to the end of fusion in the objects' interiors. If this graph was extended far into the future we would see all the brown dwarfs continue to cool. Note that even small objects around of 13Mj will increase slightly in temperature as they burn a minimal amount of fuel. The first initial much smaller bump is a result of heating as they gravitationally contract before becoming degenerate.

The initial radius of a brown dwarf is very dependent on its initial mass. As may be expected, objects of higher mass start with a much higher radius as they begin to compress to a smaller size due to gravitational forces. There is a brief period where their radius will stabilize while internal fusing occurs, as a result of radiative pressure to equaling the compressing force of gravity. When the atomic fuel has been completely burned, or the brown dwarf no longer has sufficient mass to maintain fusing, it will continue to cool and compress to a radius on the order of 1 R_J . All objects will contract to a similar size due to the mass radius relationship at this density, a result of the degeneracy in the internal structure.

Approximate equations governing these relationships between mass, radius, luminosity, temperature and time during the post-fusion lifetime were introduced in Burrows and Liebert (1993) as power laws for solar metallicity objects and are as follows:

$$L \sim 4 \cdot 10^{-5} L_{\odot} \left(\frac{10^9 \text{ yr}}{t} \right)^{1.3} \left(\frac{M}{0.05 M_{\odot}} \right)^{2.64} \left(\frac{\kappa_R}{10^{-2} \text{ cm}^2 \text{ g}^{-1}} \right)^{0.35} \quad (1)$$

$$T_{eff} \sim 1550 \text{ K} \left(\frac{10^9 \text{ yr}}{t} \right)^{0.32} \left(\frac{M}{.05 M_{\odot}} \right)^{0.83} \left(\frac{\kappa_R}{10^{-2} \text{ cm}^2 \text{ g}^{-1}} \right)^{.088} \quad (2)$$

$$M \sim 35 M_J \left(\frac{g}{10^5} \right)^{0.64} \left(\frac{T_{eff}}{1000 \text{ K}} \right)^{0.23} \quad (3)$$

$$t \sim 1.0 G \text{ yr} \left(\frac{g}{10^5} \right)^{1.7} \left(\frac{1000 \text{ k}}{T_{eff}} \right)^{2.8} \quad (4)$$

$$R \sim 6.7 \cdot 10^4 \text{ km} \left(\frac{10^5}{g} \right)^{0.18} \left(\frac{T_{\text{eff}}}{1000\text{K}} \right)^{0.11} \quad (5)$$

Where g is equal to the surface gravity, and κ_R is the average atmospheric Rosseland mean opacity. As previously mentioned, these equations are used to model the objects after their temperature increase, as its apparent they follow a power law in their extended cooling phase. Its also interesting to note that the opacity has an extremely minimal effect on the effective temperature over time. We see that all these variables are dependent on one another through this cooling process.

When observing brown dwarfs they are traditionally grouped into four spectral classes. The first we will talk about here is called M class the strongest lines in an M class dwarf are, which are titanium oxide (TiO) and vanadium oxide (VO). This is the warmest possible spectral class and emits primarily in the infrared. Because of this, not only can massive brown dwarfs be labeled in the M spectral class, but so can the smallest stars.

The next warmest spectral classification is the L class. L dwarfs are believed to have an effective temperature between 1300 and 2100 degrees kelvin. What sets them apart from other objects at this temperature, specifically M dwarfs, is the lack of TiO and vanadium oxide VO absorption lines. Instead, metal hydrides such as iron hydride (FeH) and calcium hydride (CaH) are the prominent absorptions. There is also an abundance of neutral alkali metals in the form of sodium, potassium, and cesium.

The next spectral class, T dwarf, is characterized by the appearance of CH₄, or methane. It can be said with confidence that all objects labeled as a T dwarf are also brown dwarfs. They lose the distinct hydride lines that define an L dwarf, and instead

gain much more significant absorption features from Na and K. The T dwarf class tends to radiate at a T_{eff} between 900 to 1300 Kelvin.

The last and most recently defined spectral class, class Y, occurs when ammonia (NH_3) occurs in the near infrared. It was not until 2010 when ultracool brown dwarfs were discovered that another class was needed. With temperatures less than 500 Kelvin, these objects have formed like a star but may have not fully fused all available deuterium. More recently NASA's Wide-field Infrared Survey Explorer (WISE) has discovered over ten more Y brown dwarfs, some of which are on the scale of room temperature.

A brown dwarf's spectral class is dependent on where in its lifetime the object is. As they cool with time, objects will begin their life in the M spectral class, and cool to the preceding spectral classes, L, T, then Y. Objects that may be mistaken for planets will most likely be further in their cooling process in the T or Y classes.

One of the most interesting things about a brown dwarf is that they are not in fact brown! Due to the fact that broadened sodium D lines dominate the spectra for all brown dwarfs, it has been calculated that they will actually be red to purple as a consequence of the aforementioned Na D line, as well as the other alkalis in the atmosphere. As mentioned in Burrows et al (2001) a program was used to convert a L5 brown dwarf spectrum into visible color, where it appeared magenta. It is then somewhat comical that what has been named brown, is deceptively more vivid.

The last item to discuss is how these brown dwarf objects can end up in a planetary system. The primary way this is believed to occur is a binary formation. As a star is forming in the galactic nebula, a brown dwarf can be forming in its sphere of influence. Although the star and brown dwarf may have formed in unison, the large mass difference can result in a relatively still star being orbited by a small brown dwarf.

To briefly recap, a objects that forms via gravitational collapse will exhibit many of the same features as a star during the beginning of its lifetime. This close relation to star formation means the initial metallicity of the galactic nebula can be traced throughout its lifetime. As they continue to contract, deuterium fusing can occur, resulting in a brief increase in temperature and a brief halt in contraction. After using all available deuterium, the consequence of not being massive enough to ignite hydrogen means these objects will continue to contract and cool.

3.0 Core Accretion models

The core accretion model aims to explain giant planet formation, beginning with a seed core, around a protostar. Planets will form in the protoplanetary disk during which time the star continues to accrete material. This process can result in large gas planets, potentially up to a mass on the order of $13M_J$, that can partially or fully fuse all available deuterium. It is at this point where some definitions of brown dwarf and large planets tend to blur.

A typical protoplanetary disk is thought to have a composition of 99% hydrogen and helium gas with the last 1% being “metals,” here defined as anything heavier than helium, found as solid grains of dusts of about 1 micrometer in diameter. This latter population results in the beginnings of core formation. As the solids in the disk begin to settle to the system mid-plane, these dust particles will oscillate in the z direction, leading to collisions between the particles. Its believed that this occurs most commonly outside the frost line, where there will be a higher abundance and density of solid material.

Due to the higher mass of dust in comparison to the surrounding gas, these particles endure a drag force defined by this equation given in Chambers (2010).

$$F_{drag} = -\left(\frac{\rho_{gas} c_s}{\rho R}\right) M (v - v_{gas}) \quad (6)$$

Where ρ_{gas} and c_s are the density of the gas and the speed sound in the gas respectively. While M is the mass of the dust grain, v is the speed of the grain, and v_{gas} is

the speed of the surrounding gas. The density of the grain is expressed as ρ , and R is the radius of said grain.

This force creates a headwind on the dust, causing it to fall radially inward to either the protostar, or towards the local pressure maximum. This creates a migration of heavier particles towards similar locations that results in a further increase of collisions between like sized dust grains. Laboratory experiments demonstrate that small grains, on the order of the aforementioned micrometer, will stick together after a collision at low velocity. This is a result of the electrostatic forces being strong enough to stick the two particles together (Poppe et al 2000). At high velocity the objects will elastically collide, but due to the similar motion of heavier particles in the disk, most grains will have a small relative velocity to one another.

This growth continues via collisions, now with larger objects absorbing smaller ones, until they reach a diameter of ~ 1 meter where collisions become much more destructive. From this point the physics is rather shaky, where simulations suggest that collisions may be more destructive than constructive, and there is some question as to how they continue to grow. Some progress has been made in this regard, which is discussed in Windmark et al (2012). Regardless of the process of which it occurs, the solid rock seeds continue to grow in size.

Once the planetary embryos reach a diameter of 1 km to 1000 km they gain a gravitational force that assists in gaining more mass. At this stage they are called planetesimals, and can be considered an embryo to form a planet. The next stage of the growth process is called runaway, or oligarchic growth. With the assumption that many

planetesimals have formed in the planetary disk, high velocity collisions will now lead to fragmentation, while low velocity collisions will result in a net growth of the embryo. These slow collisions between two objects results in a debris field, as well as growth dictated by the equations below:

$$\frac{M_{largest}}{M_{target} + M_{projectile}} \simeq 0.5 + s \left(1 - \frac{Q}{Q_D^*} \right) \quad (7)$$

The surviving object has a mass equal to the left side of the equation, where $M_{largest}$ equals the larger initial object, and beneath that is the sum of the two colliding objects. S is believed to be about 0.5 (Benz and Asphaug 1999) Q_D^* is the energy per unit target mass required to break up the initial body and the reassembled body contains half the mass of the target object, and Q is the kinetic energy of the projectile per target mass.

As mentioned before, the end product is a larger planetesimal and a debris field, which can be accumulated again as the object travels through the disk. Now that the embryo is of sufficient size to have a gravitational influence, it gains a gravitational focusing effect as it moves through the remaining dust and gas in the disk. This effectively increases its cross sectional area, and greatly influences the growth rate, expressed below.

$$\frac{dM_e}{dt} \sim R_e^2 \quad (8)$$

$$\frac{dM_e}{dt} \sim M_e^{\frac{2}{3}} \quad (9)$$

Where M_e is the mass of the embryo and R_e is the radius of the embryo. One of the most important things to note from this weak focusing limit is that the growth rate is independent of initial size, meaning that all embryos with small gravitation fields, diameter $\sim 1\text{km} - 10\text{km}$, will grow at the same rate, which will slow as it gains mass. As they grow in size however, the gravitational forces become more relevant and result in a stronger focusing limit demonstrated below:

$$\frac{1}{M_e} \frac{dM_e}{dt} = M_e^{\frac{1}{3}} \quad (10)$$

The most significant difference in this is that bigger objects will grow faster, and remove all available material for the smaller objects to grow. The initial objects that reach a diameter of about 10km first, will then grow at a runaway pace due to the increased gravitational focusing, and absorb all available dust and smaller embryos until they reach an isolation limit. The isolation limit is the mass that the embryos reach after they have gathered all available mass in their sphere of gravitational influence.

Now that we have a rocky core of approximately 10 earth masses (Pollock et al 1996), it starts to accumulate a gaseous envelope while it exists in the remaining gas nebula. This envelope consists primarily of the remaining hydrogen and helium gas in the system. It is assumed that the envelope itself forms a density gradient from the core to the remaining disk, until it has gathered enough mass to collapse down around the initial core as illustrated below.

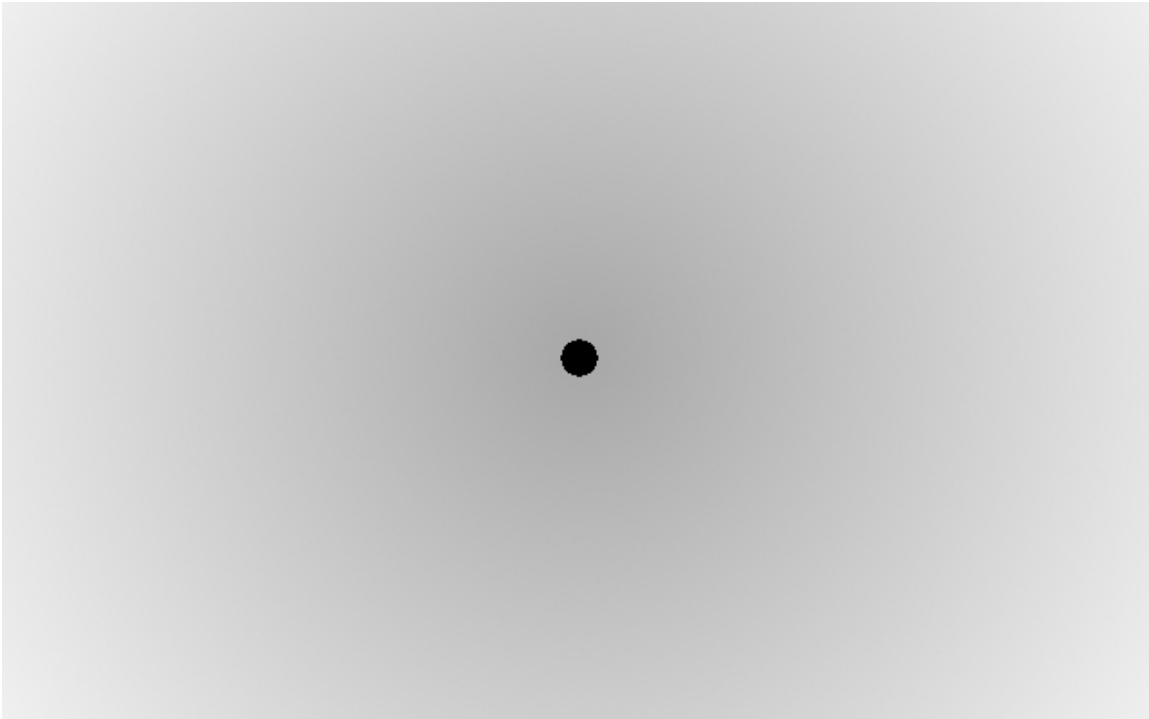


Figure 5: A simple example of an envelope gradient, where a core embryo (black circle) has accreted a gaseous envelope. Darkness represents density

As gas from the nebula falls towards the envelope there are two theories on how this occurs. The first of which, called the hot start model, suggests that the falling gas retains its thermal energy as it hits the envelope and results in hotter initial conditions. The second, called the cold start model (Marley et al 2007), suggests that falling gas releases its thermal energy as photons when it collides with the envelope, resulting in colder accreted gas and colder initial conditions. This is an important distinction, as it would suggest that objects formed via core accretion would be much cooler than brown dwarf counterparts during their early lifetimes.

The hot start model begins with a arbitrarily hot, adiabatic planet. This results in a very hot initial condition, and a rapid cooling process early in the planet's lifetime,

followed by an exponential cooling period traditionally modeled over 10 Gyr. The release of heat from the interior of the planet is related to the loss of specific entropy as shown below, which dictates the long term evolution for both models.

$$\frac{\partial L}{\partial m} = -T \frac{\partial S}{\partial t} \quad (11)$$

Where L is the luminosity, T is the temperature of the mass shell, t is time, and S is the specific entropy of the object.

This relation reveals a relatively smooth cooling process over a long period of time, seen in the figure below from Baraffe et al (2003).

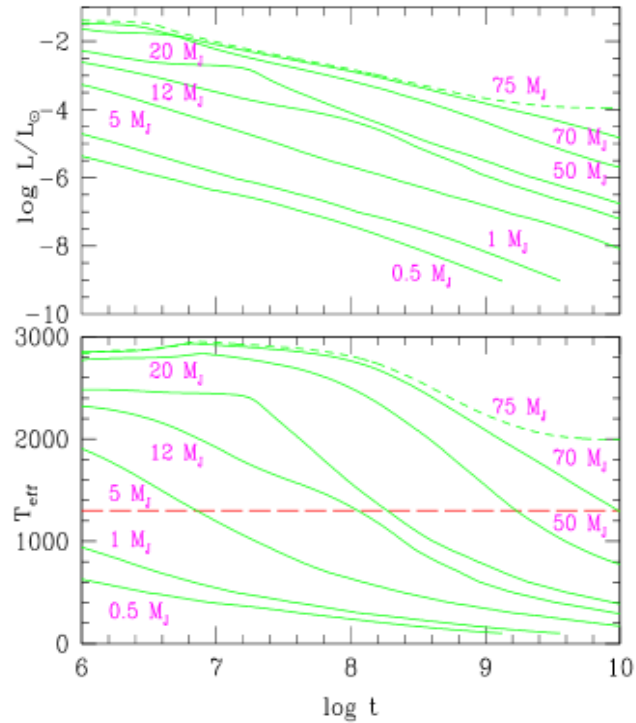


Figure 6: Time evolution of Luminosity and effective temperature for objects ranging from $75M_J$ to $0.5M_J$. The red dashed line represents $T_{eff}=1300K$.

This has been used primarily to describe gravitational instability and can be used to describe brown dwarf formation.

The cold start model first introduced by Marley et al (2007) assumes that core accretion objects do not retain all of the thermal energy from the gas accreted in the protoplanetary nebula. The major assumption is gas colliding with an atmospheric envelope will experience a shock, releasing most of, if not all of its internal entropy. This results in an object with much lower initial temperature, radius, and luminosity. The following figure, taken from Marley et al (2007), displays this cold start model as a comparison to the traditional hot start.

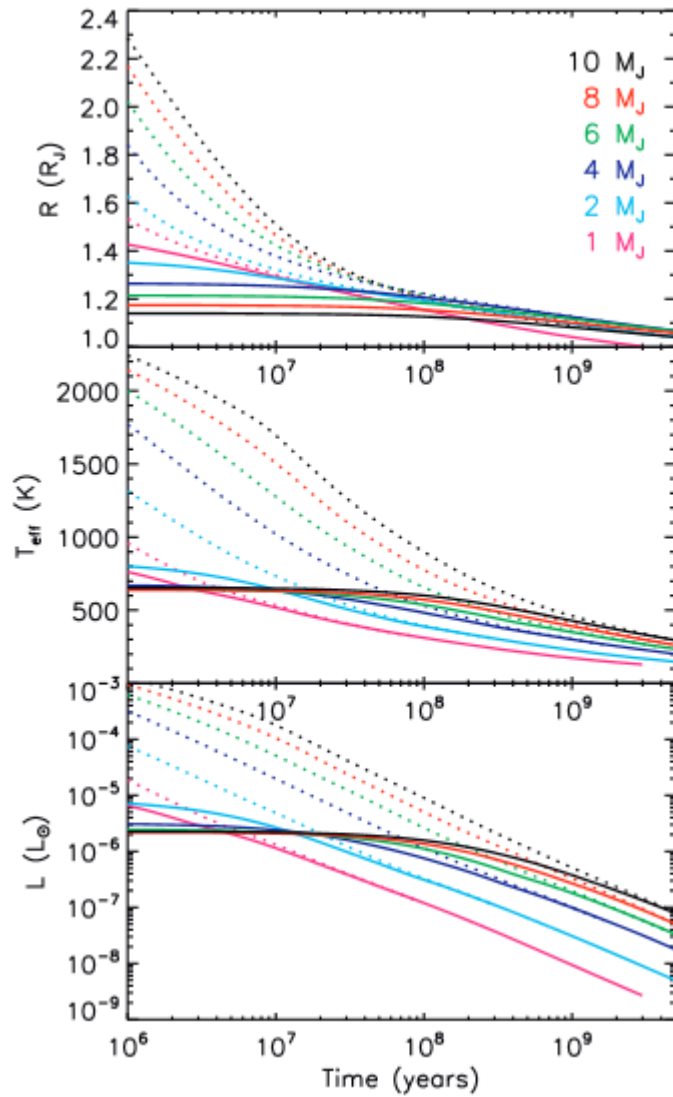


Figure 7: The time evolution of sub stellar objects using both cold start and hot start models. Top is the radius evolution, middle is the Temperature evolution, the bottom shows the Luminosity transformation.

This figure shows the evolution of both the hot start and cold start models. The first implication of this, is that the cold start core accreted models will have a lower temperature during the early lifetimes than their hot start brethren. This may become a

useful tool to determine the initial starting conditions of an object younger than 100 million years.

These two models will prove to be very important in observing stellar objects in attempt to determine their initial formation conditions.

The lifetime of a core accreted planet can then be explained in a few different stages. First is the creation of a core in a protoplanetary disk. Once it reaches a size to gain gravitational influence, it will gather adjacent embryos until it has cleared its local sphere of influence when it will reach a size of about 10 earth masses. Finally it will continue to gather hydrogen and helium from the surrounding nebula to form a final planet ranging from 1 M_J to perhaps 10 or 20 M_J .

3.0 Observations

Now that we better understand the differences between core accretion and gravitational instability formation models we can use the knowledge gathered to apply to observations of stellar objects. Knowing evolutionary models and observing an objects atmosphere and spectrum, can shed light on its initial formation conditions. This in turn, can tell us whether the object has formed via gravitational instability or core accretion.

3.1 Observation of Core Accreted Objects

As explained in the last section, cold start should have a cooler effective temperature than their hot start alternatives. This means if the age of an object can be determined independent of its temperature, the T_{eff} and age can be used to match up to evolutionary models to determine its initial formation conditions. This is a rare case however, as many times the temperature of the object will be used to derive how old the object is.

Looking at the objects in our own solar system can give us clues to how objects outside of it can look. For our two core-accreted gas giants, Saturn and Jupiter, the Galileo and Cassini experiments showed that they have significantly more metals than the sun. The increased metallicity in comparison to the parent star is believed to exist for exoplanets as well. With this in mind, an observation of an object with increased metallicity greatly implies that it has formed inside a protoplanetary disk via core-

accretion. Young gas planets with more metals than their host star have been modeled by Fortney et al (2008) and have been shown to have a smaller radius than similar objects of less metal content. This smaller radius can provide a hint to an objects interior content.

This need for a greater amount of metals to create a core-accreted planet has resulted in an observational planet-metallicity correlation that indicates there is an increase in planet frequency around a parent star with greater metallicity. This strongly suggests that core-accretion is the primarily method of planet formation because of the required solid and ices to form an initial core exist in abundance around these more metal rich hosts.

With the release of more microlensing data in addition to long term radial velocity data, it has been observed that more gas giants exist outside the ice line, which may also hint at planet formation scenarios.

The next step in observation of these objects is direct imaging. Although the current generation of telescopes is not able to sufficiently image these objects, there are some potential candidates that stand out for the next generation. Particularly is star HR8799 which has a system of four planets. Each planet orbits the parent star, and exists well below the deuterium fusing mass. Directly imaging these planets, or similar objects can give a baseline model for what exoplanet atmospheric spectra can look like.

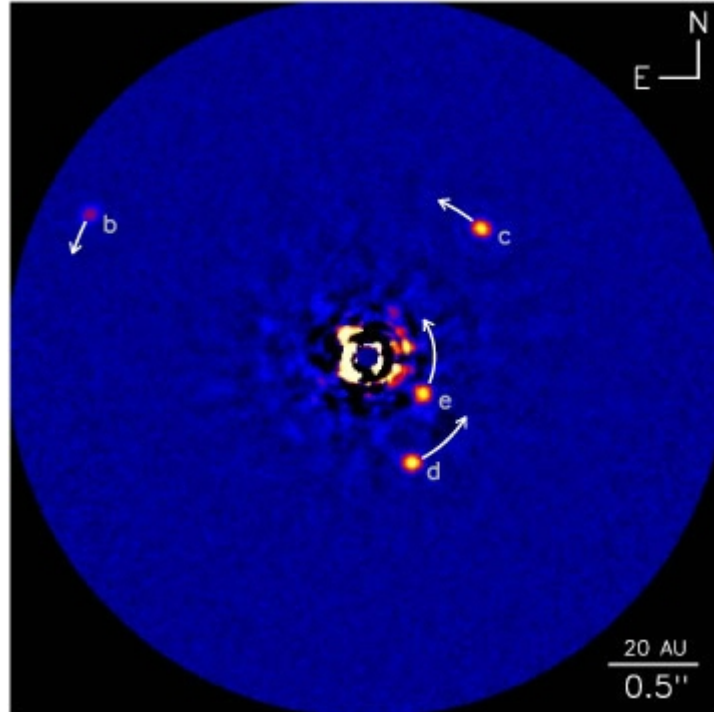


Figure 8: The HR 8799 system. The brightness of the host star, and large semi major axes should make it a good candidate for planetary imaging.

The next telescope to be able to potentially achieve similar images is called the Gemini Planet Imager and will be operational for extended use in April of 2014. The goal of the project is to directly image extrasolar planets in the southern hemisphere.

3.2 Observations of Brown Dwarfs/Gravitational Collapse

Traditional brown dwarfs form in the same manner of stars, and therefore share many observational qualities with their larger brethren. The Wide Infrared Survey Explorer, or WISE, telescope probed young star formation areas and found many brown

dwarfs forming in the same fields. All the WISE observational data suggests that brown dwarfs and stars form in the same manner.

What follows is the equation for the stellar initial mass function (IMF) from Salpeter (1955):

$$\frac{dN}{d \log M} = \phi_t(M_v) \quad (12)$$

This equation is used to describe the number of stars, N , that result from a cloud of mass M . This is equal to the luminosity function of absolute visual magnitude $\phi_t(M_v)$. Below is a comparison of an IMF model in comparison to the WISE observational data from Chabrier et al (2014).

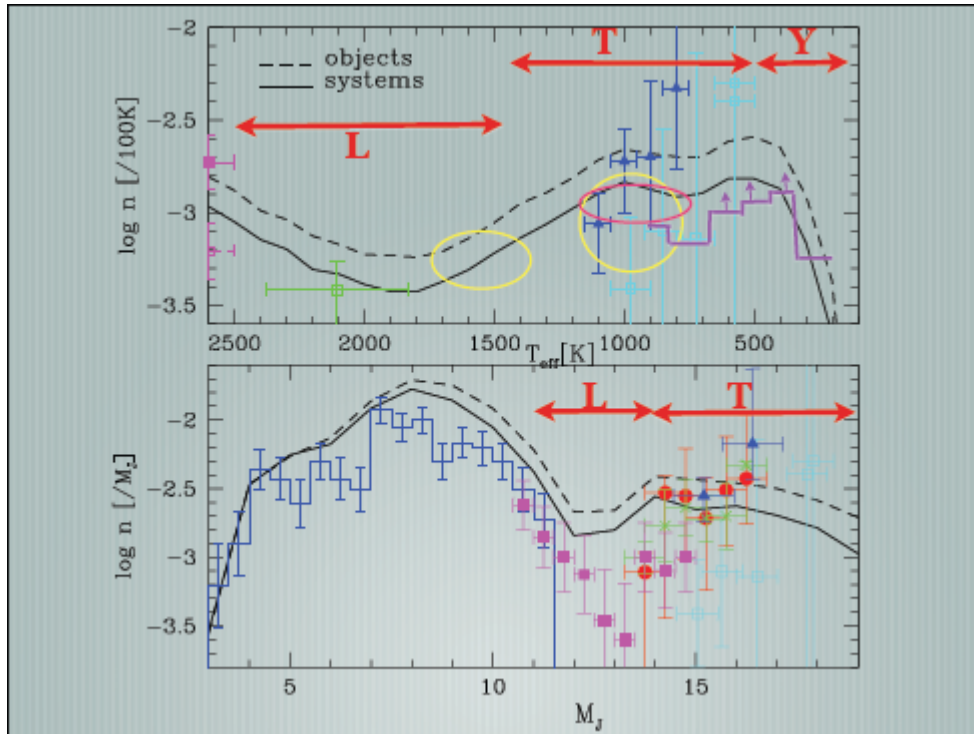


Figure 9: Brown dwarf density as a function of T_{eff} and M_J respectively. The dashed line represents the initial mass function for resolved object, while the solid line represents unresolved binary systems. L, T, Y show spectral classes of the objects. The triangles, squares, and circles are various observations, while the histogram with arrows represents newer WISE data.

The data found by WISE suggests that the tail end of star formation processes continue to masses as low as $5 M_J$.

Perhaps one of the best objects to study to get a high quality baseline spectrum for smaller brown dwarfs is Luhman 16. Luhman 16 a binary brown dwarf system with a two objects of about $30M_J$. This is the closest brown dwarf to earth, and as a result can be a good object to further pursue the study of brown dwarf atmospheres and their composition.

4.0 Conclusion

Given the discussion of this paper, clear definitions between a large gas planet and a brown dwarf need to be established. Currently the definition is a mass limit of $13M_J$, where deuterium begins to fuse, however this mass boundary depends on some degree of compositional and evolutionary history. Most importantly, there is on is a clear mass overlap between the two kinds of objects and a distinct limit is a problematic way to determine the difference.

Deuterium fusing is possible in a core accreted object, or an object forming via gravitational instability. This limits its usefulness in distinguishing the two objects.

The defining factor to determine the difference between a brown dwarf and a planet should be its initial formation conditions. An object that forms like a star, via gravitational collapse of a a small portion of a molecular cloud should be considered a brown dwarf. An object that forms via core accretion in a proto-planetary disk should be considered a giant gas planet, regardless of final mass.

This is an important distinction as a $11M_J$ core-accreted planet will have more in common with a $13M_J$ core accreted planet than a $11M_J$ gravitationally collapsed brown dwarf.

This is not an easy task to do at first glance, however it should become substantially easier with the next generation of telescopes. The increased technology will allow astronomers to take a spectrum of newly discovered objects, where the degree of metallicity enhancement should be used to determine its initial formation conditions.

Acknowledgments

I wish to thank Professor Jonathan Fortney, my thesis adviser, without his guidance this paper would be arguably be incoherent. I would also like to thank Professor Adriane Steinacker for her assistance in providing the positive encouragement to finish this milestone.

REFERENCES

- Baraffe, I; G. Chabrier; T. Barman; F. Allard; P. H. Hauschildt. *Astron. & Astrophys.* **v402** 2003
- Benz, W.; E. Asphaug. *Icarus.* **v142** 1999
- Bodenheimer, Peter; Genarro D'Angelo, Jack J. Lissauer; Jonathan J. Fortney; Didier Saumon. *Astrophysical J.* **v770** 2013
- Burrows, Adam; J. Liebert. *Reviews of Modern Physics.* **v65** 1993
- Burrows, Adam; W. B. Hubbard; J. I. Lunine; James Liebert. *Reviews of Modern Physics.* **v73** 2001
- Chabrier, G.; I. Baraffe; F. Allard; P. Hauschildt. *Astrophysical J.* **v542** 2000
- Chabrier, G.; I. Baraffe; F. Selsis; T. S. Barman; P. Hennebelle; Y. Alibert. *Protostars and Planets V.* 2005
- Chabrier, G.; A Johansen; Mjanson; R. Rafikov. *Protostars and Planets VI.* 2014
- Chambers, John. *Exoplanets.* 2010
- Fortney, Jonathan; M. S. Marley; D. Saumon; K Lodders. *Astrophysical J.* **v683** 2008
- Guillot, Gristan. *Physics Today.* **April** 2004
- Kumar, Shiv S. *Astrophysical J.* **v137** 1963
- Leconte, Jeremy; Gilles Chabrier. *Astron. & Astrophys.* **v540** 2012
- Marley, Mark S.; Jonathan J. Fortney; Olenka Hubickyj; Peter Bodenheimer; Jack J. Lissauer. *Astrophysical J.* **655** 2007
- Molliere, P.; C. Mordasini. *Astron. & Astrophys.* **v547** 2012
- Nakajima, T.; B. R. Oppenheimer; S. R. Kulkarni; D. A. Golimowski; K. Matthews; S. T. Durrance. *Nature.* **v378** 1995
- Oppenheimer, B. R.; S. R. Kulkarni; K. Matthews; T. Nakajima. *Science.* **v270** 1995
- Pollack, J. B.; O. Hubickyj; P. Bodenheimer; J. Lissauer; M. Podolak; Y. Greenzweig. *Icarus.* **v124** 1996
- Poppe, T.; J. Blum; T Henning. *Astrophysical J.* **v533** 2000
- Salpeter, Edwin E. *Astrophysical J.* **v121** 1955
- Schneider, Jean; Cyril Dedieu; Pierre Le Sidaner; Renaud Savalle; Ivan Zolotukhin. *Astron. & Astrophys.* **v532** 2011
- Spiegel, David S.; Adam Burrows; John A. Milsom. *Astrophysical J.* **v727** 2011
- Stevenson, David J. *Icarus.* **v62** 1985
- Stevenson, David J. *Annual Review of Astron. & Astrophys.* **v29** 1991
- Stevenson, David J. *Physics Today* **April** 2004
- Windmark, F.; T. Birnstiel; C. W. Ormel; C. P. Dullemond. *Astron. & Astrophys.* **v548** 2012